ORGANIC LETTERS

2011
Vol. 13, No. 16
4188–4191

Highly Chromic, Proton-Responsive Phenyl Pyrimidones

Jyothi Dhuguru, Chirag Gheewala, N. S. Saleesh Kumar, and James N. Wilson*

Department of Chemistry, University of Miami, 1301 Memorial Drive, Coral Gables, Florida 33124, United States

jnwilson@miami.edu

Received June 3, 2011

ABSTRACT

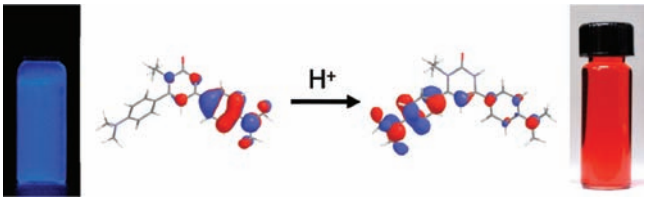

Aryl pyrimidones are pharmacologically relevant compounds whose optical properties have only been partially explored. We report the synthesis and optical characterization of a series of aryl- and diaryl-2(1*H*)-pyrimidones. The electronic transitions of these chromophores are modulated by the extent of conjugation between the pendant phenyl ring and the pyrimidone core as well as the presence of electron-donating auxochromes. Monoprotonation of the pyrimidone ring results in large hyperchromic and bathochromic shifts as well as switching of fluorescence making these phenyl pyrimidones of interest as sensory materials.

The pyrimidone moiety is one of the most prevalent, biologically relevant heterocycles; it is featured prominently in nucleic acid chemistry[1] and in many pharmacologically active compounds.[2] In the latter context, aryl-substituted pyrimidones have been examined as kinase inhibitors, antimicrobials, and analgesics.[3] The hydrogen bonding pyrimidone core coupled to a hydrophobic aryl substituent promotes several modes of interaction in binding to a biomacromolecular target. This structural motif also makes arylpyrimidones of interest as optically active materials, particularly for the 4-aryl and 4,6-diarylpyrimidones.

Only a few reports have investigated their photophysical properties.[4,5] Wu et al.[4] examined a series of asymmetric 4,6-diarylpyrimidones and identified a Zn^{2+} responsive ligand; coordination of the metal ion via the pyrimidone core resulted in an increase in fluorescence. This behavior may be extended to the arylpyrimidones with biological activity provided interactions with the pyrimidone moiety, such as protonation or hydrogen bonding, induce a similar optical response. For example, Shafer et al.[3a] recently reported a family of 4, 6-diarylpyrimidone-based inhibitors of CDC7 serine/threonine kinase with nanomolar affinities. These extended aromatic frameworks suggest the possibility of self-reporting ligands, provided a distinct optical response is generated upon binding.

To gain insights into the optical properties of arylpyrimidone constructs and their response to protonation, we have synthesized a family of "double armed" 1-ethyl-4,6-diphenyl-2(1*H*) pyrimidones (**1c**, **2c**, and **3c**, Figure 1) and their "single-arm" derivatives, 1-ethyl-4-phenyl-2(1*H*) pyrimidones and 1-methyl-6-phenyl-2(1*H*) pyrimidones (**1a**, **1b**, **2a**, **2b**, **3a** and **3b**). The absorption and emission wavelengths are modulated through substitution to the aryl

(1) (a) Wang, G.; Tam, R. C.; Gunic, E.; Du, J.; Bard, J.; Pai, B. *J. Med. Chem.* **2000**, *43*, 2566–2574. (b) Winkley, M. W.; Robins, R. K. *J. Org. Chem.* **1969**, *34*, 431–434. (c) Chun, B. K.; Song, G. Y.; Chu, C. K. *J. Org. Chem.* **2001**, *66*, 4852–4858.

(2) (a) Zhu, Y.-F.; Guo, Z.; Gross, T. D.; Gao, Y.; Connors, P. J.; Struthers, R. S.; Xie, Q.; Tucci, F. C.; Reinhart, G. J.; Wu, D.; Saunders, J.; Chen *J. Med. Chem.* **2003**, *46*, 1769–1772. (b) Zhang, Z.; Wallace, M. B.; Feng, J.; Stafford, J. A.; Skene, R. J.; Shi, L.; Lee, B.; Aertgeerts, K.; Jennings, A.; Xu, R.; Kassel, D. B.; Kaldor, S. W.; Navre, M.; Webb, D. R.; Gwaltney, S. L. *J. Med. Chem.* **2010**, *54*, 510–524.

(3) (a) Shafer, C. M.; Lindvall, M.; Bellamacina, C.; Gesner, T. G.; Yabannavar, A.; Jia, W.; Lin, S.; Walter, A. *Bioorg. Med. Chem. Lett.* **2008**, *18*, 4482–4485. (b) Prasad, Y. R.; Rajasekhar, K. K.; ShankarananthV.; Maulaali, S. C.; Kumar, G. S. S. P.; Reddy, K. N. *J. Pharm. Res.* **2010**, *3*, 2291–2292. (c) Keri, R. S.; Hosamani, K. M.; Shingalapur, R. V.; Hugar, M. H. *Eur. J. Med. Chem.* **2010**, *45*, 2597–2605.

(4) Nishio, T.; Omote, Y. *J. Chem. Soc., Perkin Trans. 1* **1984** 239–242.

(5) Wu, H.; Chen, X.-m.; Wan, Y.; Ye, L.; Xin, H.-q.; Xu, H.-h.; Pang, L.-l.; Ma, R.; Yue, C.-h. *J. Chem. Res.* **2008**, 711–714.

10.1021/ol2014945
Published on Web 07/26/2011

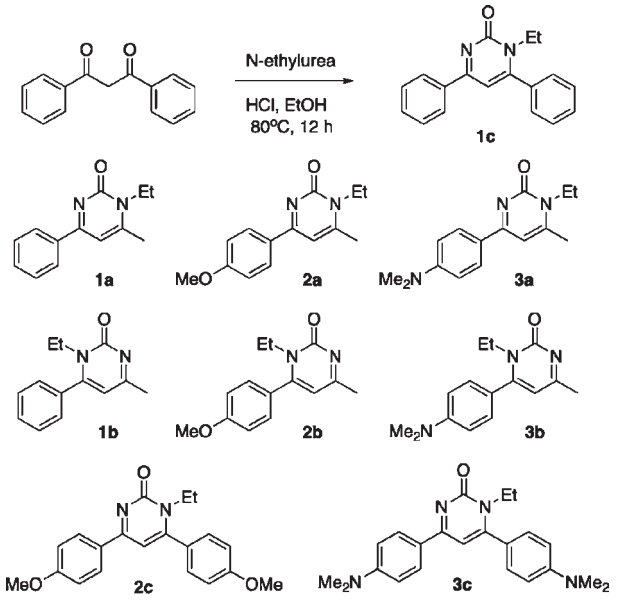

Figure 1. Structures of phenylpyrimidones **1a**–**3c** and representative synthesis of **1c**.

arms, and the diaryl compounds in particular show a strong chromic and emission response upon protonation.

1a–**3c** were synthesized via acid-catalyzed condensation of ethylurea with the appropriate diketone (Figure 1).[6,7] The single arm 4-phenyl-pyrimidone and 6-phenyl-pyrimidone isomers were isolated from the same reaction and separated by column chromatography. Use of an alkyl urea allows evaluation of the unique isomers, avoiding tautomeric equilibria. Yields were moderate, ranging from 36% (both isomers) in the case of **1a** and **1b** (25% and 11%, respectively) to 19% in the case of **2c**. The crystalline solids appeared colorless (**1a**–**c**) to bright yellow (**3a**–**c**) demonstrating the effect of the electron-donating methoxy and dimethylamino auxochromes on the arylpyrimidone core.

Identification and structural assignment of the isomers were made on the basis of ^{1}H NMR and 1D-NOE spectra. Density functional calculations at the 6-31G* level (M06 basis set)[8] reveal that the pendant phenyl substituent is twisted in the case of the 6-phenyl-pyrimidones (**1b**, **2b**, **3b**), while, in the case of the 4-phenyl-pyrimidones (**1a**, **2a**, **3a**), the aromatic framework is essentially planar. Thus, the chemical shifts of the aromatic protons, H_a and H_b (shown for **1a** and **1b**, Figure 2), are expected to vary as a function of aromatic ring current.[9] Inspection of the aromatic region of the ^{1}H NMR spectra of **1a** and **1b** reveals that

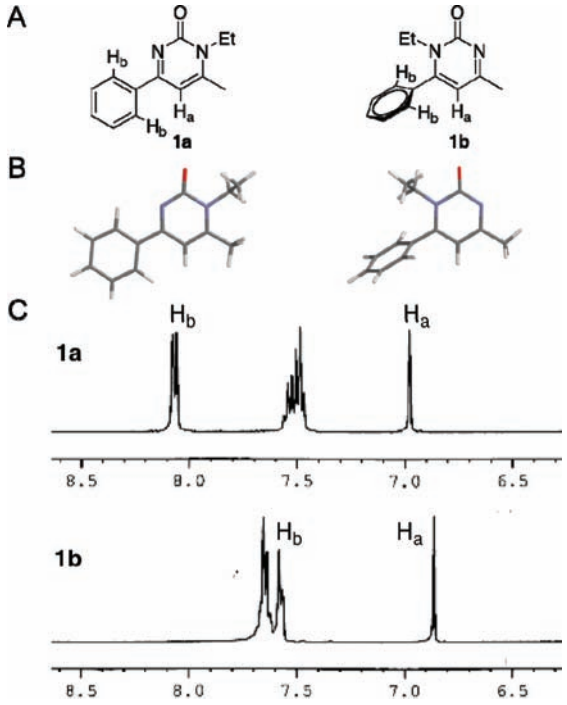

Figure 2. Structural assignment of 4-phenyl- and 6-phenyl-2(1*H*)-pyrimidone isomers based on optimized geometries (DF 6-31G*) and ^{1}H NMR spectra.

for **1a** the protons H_a are shifted downfield by 0.13 ppm relative to **1b**. The electron-withdrawing nature of the pyrimidone core exerts an additional effect in the planar aromatic system of **1a**, leading to increased deshielding of H_b protons that are shifted even further downfield by 0.50 ppm relative to **1b**. 1D-NOE spectra confirm the assignment of the two isomers: irradiation of the α-carbon protons of the N-ethyl substituent reveals an NOE on the adjacent 6-methyl group for **1a**; for **1b**, the effect is observed on the phenyl protons, H_b (see Supporting Information).

We investigated **1a**–**3c** by UV–vis and fluorescence spectroscopy to determine how conjugation between the pendant aryl arms and the pyrimidone core may influence the optical properties of the chromophores. We also obtained spectra in the presence of TFA to examine the effects of monoprotonation at N3[10] on the optical response of these aromatic molecules. The steric interference between the 6-phenyl and N-ethyl substituents of **1b**, **2b**, and **3b** results in a twisted geometry modulating the interaction of the two aromatic rings, while, in the case of **1a**, **2a**, and **3a**, the π-systems of pyrimidone and phenyl rings should exhibit greater overlap; these effects may be reflected in the optical spectra with changes in $\lambda_{max,\ abs}$ or ε. Also of interest was the relative contribution or interaction of the two arms in the diphenyl derivatives, **1c**, **2c**, and **3c**.

(6) George, S.; Nangia, A.; Bagieu-Beucher, M.; Masse, R.; Nicoud, J.-F. *New J. Chem.* **2003**, *27*, 568–576.
(7) Shavaleev, N. M.; Scopelliti, R.; Gumy, F.; Bünzli, J.-C. G. *Eur. J. Inorg. Chem.* **2008**, *2008*, 1523–1529.
(8) Zhao, Y.; Truhlar, D. *Theor. Chim. Acta.* **2008**, *120*, 215–241.
(9) Mitchell, R. H.; Iyer, V. S.; Khalifa, N.; Mahadevan, R.; Venugopalan, S.; Weerawarna, S. A.; Zhou, P. *J. Am. Chem. Soc.* **1995**, *117*, 1514–1532.
(10) (a) Kasende, O.; Zeegers-Huyskens, T. *J. Mol. Struct.* **1981**, *75*, 201–207. (b) Shoffner, J. P.; Bauer, L.; Bell, C. L. *J. Heterocycl. Chem.* **1970**, *7*, 479–485.

The spectra for **1a**–**3c** are depicted in Figure 3 with Table 1 summarizing the key spectral parameters ($\lambda_{max,\ abs}$, ε, $\lambda_{max,\ em}$, Φ_{em}). Several trends are apparent that reflect the effects of the auxochromes as well as the molecular topology (i.e., 4,6-diphenyl vs 4-phenyl vs 6-phenyl derivatives); the 4,6-diphenylpyrimidones are presented first with the relative contributions of the two "arms" discussed below. The most pronounced spectral features are the bathochromic shift of $\lambda_{max,\ abs}$ and hyperchromicity observed upon introduction of TFA. For example, **3c** appears colorless in CH_2Cl_2 and transforms to deep red when exposed to TFA (Figure 3D). The bathochromic shift was largest for **3c** (126 nm), with a moderate shift for **2c** (77 nm) and only a slight shift for **1c** (17 nm) correlating well with the presence and relative strength of the electron-donating substituents. Conversely, **1c** exhibits the largest enhancement of ε (nearly 3-fold), while **2c** and **3c** exhibit 2- and 1.5-fold increases, respectively. Marked changes in fluorescence were also observed upon introduction of TFA. While **1c** and **2c** were weakly or nonemissive in CH_2Cl_2 solutions, addition of TFA resulted in a significant enhancement of fluorescence; for **2c** a 30-fold increase in Φ_{em} was observed. Conversely, **3c** displays a Φ_{em} of 0.49 in CH_2Cl_2 with exposure to TFA quenching the emission. The absorption spectra of the 4-phenyl and 6-phenyl derivatives (Figure 3B and 3C) reveal that the electronic transitions of the diphenyl derivatives more closely resemble those found for the 4-phenyl than for the 6-phenyl derivatives based on the position of $\lambda_{max,\ abs}$ as well as the magnitude of the bathochromic and hyperchromic shifts (Table 1).

The molecular basis for the observed spectral behavior is not immediately apparent. While the bathochromic shifts are most likely the result of a decrease in the HOMO–LUMO gap, the physical basis for the hyperchromicity is not clear. Protonation may serve to enhance the electron-withdrawing nature of the pyrimidone core lowering the LUMO and producing an intramolecular charge transfer-like absorption. However, polarization of the HOMO and LUMO is associated with low ε,[11] which is not observed in the present case. By considering the molecular orbital picture for **1a**–**3c** in the neutral and protonated forms, we gain some insights into the electronic transitions of these chromophores. The equilibrium geometry of **1a**–**3c** in the neutral and protonated forms were calculated using DFT (M06) at the 6-31G* level.[9] The energy of the calculated HOMO→LUMO transitions correlates well with the experimental values of $\lambda_{max,\ abs}$. Figure 4 depicts the LUMO and three HOMOs for **1a**–**c** in the neutral and protonated forms; similar MO levels and topologies were found for **2a**–**c** and **3a**–**c**. Each of the occupied MOs is within 1 eV and therefore likely to contribute to the optical transitions observed in the UV–vis spectrum between 250 and 375 nm. Protonation leads to a redistribution of the atomic orbital contributions to each MO. The HOMO and $HOMO^{-1}$ for neutral forms of **1a** and **1c** effectively

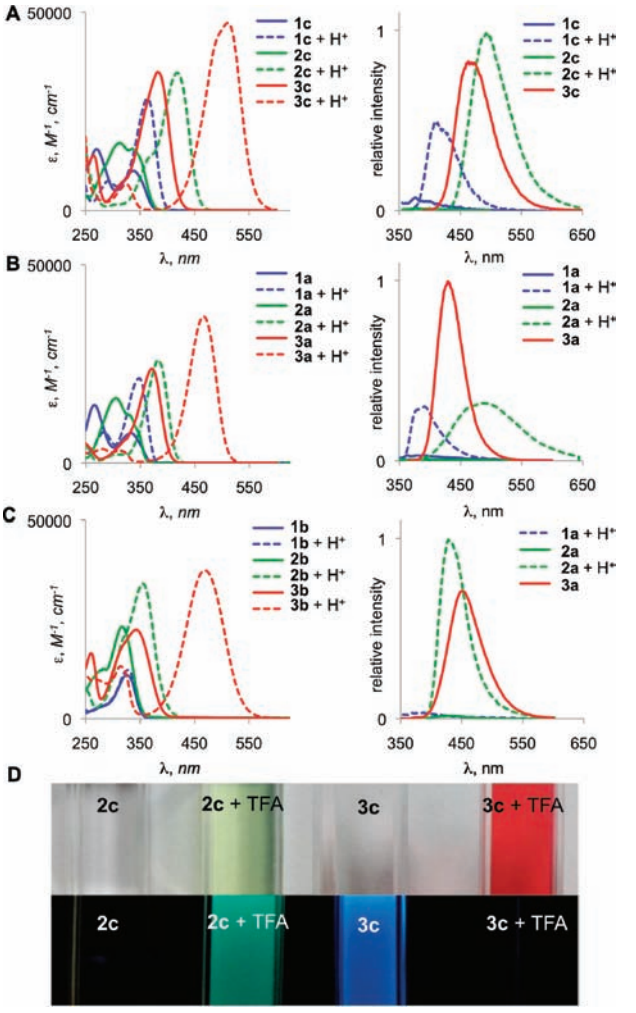

Figure 3. UV–vis and fluorescence spectra of **1a**–**3c** in CH_2Cl_2. The absorption and emission are modulated by protonation with TFA. In all cases, modest to large hyperchromic and bathochromic shifts are observed with TFA addition. For phenyl (**1a**–**1c**) and methoxyphenyl (**2a**–**2c**) derivatives, emission is enhanced by the addition of TFA; in the case of dimethylamino-substituted compounds **3a**–**3c**, emission is quenched by addition of TFA.

combine into the HOMO for the protonated forms. Thus, the nearly 3-fold enhancement of ε for the lowest energy transition can be rationalized, in part, on the basis of greater spatial overlap of the HOMO and LUMO for the protonated species. An additional contribution to the increase in ε upon protonation may arise from the $HOMO^{-2}$ to LUMO transition, which for **1a** and **1c** is calculated to be within 0.8 and 0.3 eV, respectively. For the unprotonated species, $HOMO^{-2}$ is largely σ in character and is orthogonal to the π-system resulting in poor overlap with the LUMO. On the other hand, in the protonated form, the $HOMO^{-2}$ is π in nature and possesses good overlap with the LUMO and may contribute to the high observed ε. In the case of **1b**, the lowest energy optical transition was not significantly enhanced upon TFA addition. Inspection of

(11) (a) Schulman, S. G.; Underberg, W. J. M. *Anal. Chim. Acta* **1979**, *108*, 249–254. (b) Wilson, J. N.; Bunz, U. H. F. *J. Am. Chem. Soc.* **2005**, *127*, 4124–4125.

Table 1. Photophysical Characteristics of **1a**–**3c**

compd	$\lambda_{max,\ abs}$,[a] nm	ε,[a,b] M^{-1}, cm^{-1}	E_{calc},[c] eV	$\lambda_{max,\ abs}$,[d] nm	ε,[b,d] M^{-1}, cm^{-1}	E_{calc},[c,e] eV	$\lambda_{max,\ em}$,[a] nm	Φ_{em}[a,b]	$\lambda_{max,\ em}$[d]	Φ_{em}[b,d]
1a	335	7200	5.0	348	21 000	4.5	384	0.009	389	0.14
1b	329	10 000	5.3	331	12 000	4.5	–	–	390	0.007
1c	344	9900	4.3	361	28 000	4.3	374	0.01	408	0.05
2a	335	16 000	5.0	387	25 000	4.0	375	0.01	486	0.40
2b	321	23 000	5.4	358	33 000	3.8	420	0.006	424	0.28
2c	337	17 000	4.8	414	34 000	3.7	375	0.02	488	0.62
3a	376	23 000	4.4	473	37 000	3.5	426	0.57	–	–
3b	348	22 000	4.8	474	37 000	3.2	448	0.24	–	–
3c	378	34 000	4.4	504	47 000	3.1	464	0.49	–	–

[a] CH_2Cl_2. [b] ±5%. [c] Energy of the HOMO–LUMO transition, DF MO6 6-31G*, ref 8. [d] CH_2Cl_2 with 1% TFA. [e] For the N3 protonated species.

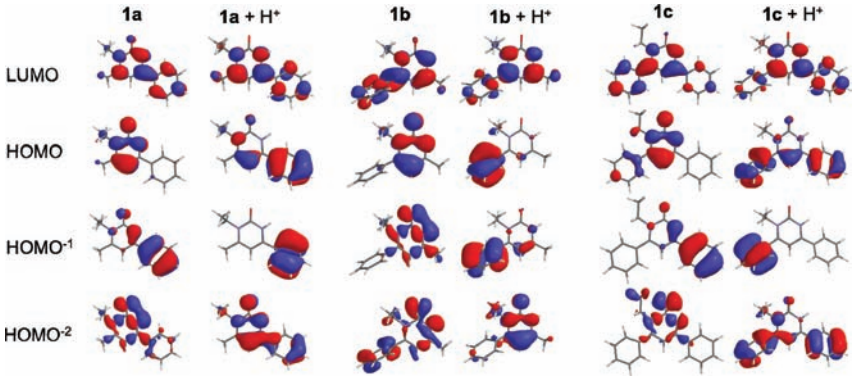

Figure 4. Molecular orbital representations for **1a**–**c**. Protonation results in a reorganization of atomic orbital contributions to the HOMO, $HOMO^{-1}$, and $HOMO^{-2}$ which may be correlated to the observed hyperchromic and bathochromic shifts on the basis of improved orbital overlap and lower energy gaps. $\Delta E_{LUMO-HOMO}$ are given in Table 1.

the HOMO through $HOMO^{-2}$ for **1b** in the protonated and unprotonated forms shows that the occupied MOs remain largely localized to either the phenyl arm or the pyrimidone core. The small increase observed for ε likely results from the diminished $n\rightarrow\pi^*$ and increased $\pi\rightarrow\pi^*$ contribution to the absorption band centered near 330 nm. The 6-phenylpyrimidone derivatives, **1b**, **2b**, and **3b**, display the lowest quantum yields in their respective series. This may also be due to the disjoint FMOs; the excited state likely exhibits more CT character that may contribute to the lower Φ_{em}.

In summary, we have synthesized and evaluated the optoelectronic properties of a series of highly chromic, proton responsive phenyl- and diphenylpyrimidones. The large hyperchromic and bathochromic shifts observed may be rationalized on the basis of the improved spatial overlap of HOMO and LUMO. Additionally, examples of both "turn-on" and "turn-off" fluorescence were observed; high overall brightness ($\varepsilon \times \Phi_{em}$) coupled with large on/off ratios makes these simple, compact fluorophores of potential interest as sensory materials. Applications of arylpyrimidone derivatives as self-reporting ligands are envisaged given the continued interest of this motif as a broadly active pharmacophore.

Acknowledgment. This research was supported by an American Cancer Society Institutional Research Grant.

Supporting Information Available. Experimental procedures and characterization data. This material is available free of charge via the Internet at http://pubs.acs.org.